NANO LETTERS

2006
Vol. 6, No. 7
1396−1400

Nanocrystal-Based Light-Emitting Diodes Utilizing High-Efficiency Nonradiative Energy Transfer for Color Conversion

Marc Achermann,[†] Melissa A. Petruska,[†] Daniel D. Koleske,[‡] Mary H. Crawford,[‡] and Victor I. Klimov*,[†]

Los Alamos National Laboratory, Los Alamos, New Mexico 87545, and Sandia National Laboratories, Albuquerque, New Mexico 87185

Received February 20, 2006; Revised Manuscript Received April 28, 2006

ABSTRACT

We report a practical implementation of high-efficiency color conversion in an electrically pumped light-emitting diode (LED) using nonradiative energy transfer. On the basis of a new LED design that offers both strong energy-transfer coupling and efficient carrier injection, we show that a hybrid structure comprising a single monolayer of CdSe nanocrystals assembled on top of an InGaN/GaN quantum well provides nearly 10% color conversion efficiency. This value is significantly higher than that for a traditional absorption–re-emission color-conversion scheme in a similar device structure. Furthermore, these hybrid devices can also provide improved efficiencies, compared not only to phosphor-based structures but also to stand-alone LEDs.

Lighting applications are responsible for approximately 20% of consumed electricity worldwide. Solid-state approaches promise not only increased efficiency of lighting devices but also improved reliability. In its traditional implementation, solid-state lighting involves a color-conversion step, in which a high-energy photon emitted by a light-emitting diode (LED) is absorbed by a phosphor that then re-emits a lower-energy photon. Significant energy savings can be obtained if the light source activates the phosphor directly via nonradiative energy transfer (ET),[1−4] which removes several of the intermediate steps involved in color conversion (e.g., emission of a primary photon, extraction of this photon from the LED, and photon absorption by the phosphor), thereby eliminating energy losses associated with these steps. Here, we demonstrate the first practical implementation of such an approach using an electrically driven InGaN/GaN quantum well (QW) that is *ET-coupled* to a single monolayer of semiconductor nanocrystals (NCs) serving as color-selectable phosphors.

The most extensively explored approach to electrical pumping of NCs in light-emitting devices involves the use of hybrid organic/inorganic blends, in which charge carriers are delivered to NCs via a network of organic molecules and the percolated NC system itself.[5−9] Such structures, however, suffer from the low electronic conductivity of both organic and inorganic device components. Improved performances can be obtained in layered structures comprising an NC monolayer sandwiched between well-defined organic hole- and electron-transport layers.[10] Recently, a new, all-inorganic LED architecture was demonstrated, in which NCs were incorporated at the p−n junction formed by GaN injection layers.[11]

A common feature of the structures in the above examples is that direct electrical contact to NCs is required, which is not easy to obtain because of the presence of the insulating molecules capping the NC surface. Furthermore, since electrons and holes are delivered to NCs separately, optimizing the performance of these devices requires balancing electron and hole injection currents. An alternative approach to activating NCs is through exciton/energy transfer.[1−4,12] Since this process relies on dipole−dipole interactions, it is not significantly inhibited by the surface passivation layer. Additionally, it automatically provides a balance between the numbers of injected electrons and holes.

A proof of principle for the "excitonic" injection mechanism was demonstrated in our recent studies, in which we utilized ET from an optically excited InGaN/GaN QW to activate emission from CdSe NCs.[4,12] In these experiments, we demonstrated that at sufficiently close NC−QW separations ET could successfully compete with both radiative and nonradiative decay in the QW, leading to high transfer efficiencies in excess of 50%. However, the practical implementation of the ET pumping scheme in an electrically

* To whom correspondence may be addressed. E-mail: klimov@lanl.gov.
[†] Los Alamos National Laboratory.
[‡] Sandia National Laboratories.

10.1021/nl060392t CCC: $33.50
Published on Web 06/16/2006

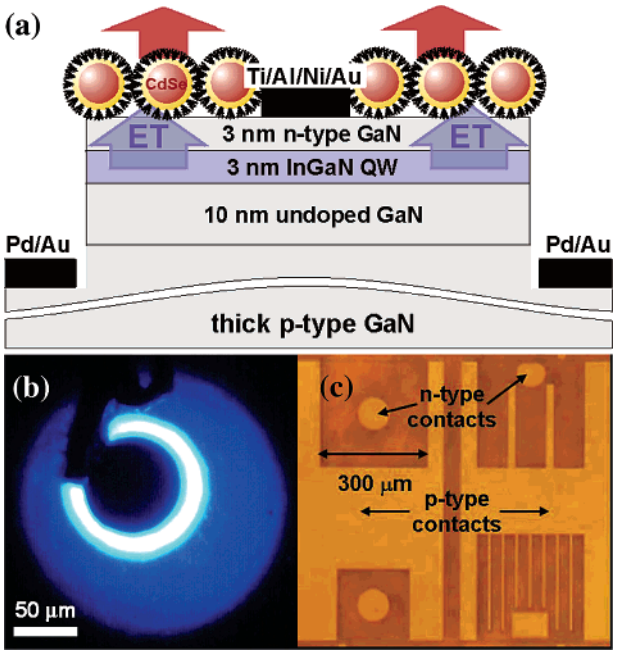

Figure 1. (a) Schematic cross section of the ET-LED structure. The 10 nm undoped GaN layer below the QW is a transition layer to provide a good interface for the QW growth. (b) ET-LED under electrical excitation. The white ring around the n-contact indicates strongest QW emission (the picture is overexposed to show the spatial extent of the LED emission). (c) Contact geometry of a real device.

driven device is complicated by two conflicting requirements. The fast reduction of the ET coupling with increasing QW−NC separation, d (coupling scales as d^{-4}; refs 4 and 12), dictates the use of exceedingly thin QW barrier layers. On the other hand, relatively thick barriers are required to reduce nonradiative carrier losses in the QW and to enhance injection efficiencies (in the case of thin barriers, the injection efficiency is reduced because of reduced carrier mobilities that limit current spreading).

As a solution to this problem, we use an inverted LED design (Figure 1a), in which we grow an InGaN QW on top of a thick, p-doped GaN barrier and complete the structure with a thin, n-type GaN cap layer (normally a QW is grown on top of the n-type layer). In this way we take advantage of the much higher mobility of n-GaN compared to p-GaN, which allows us to obtain significant current spreading despite the small thickness of the electron-injection layer. By performing direct spatial mapping of the emission intensity (Figure 1b), we observe that the QW emission extends up to ~80 μm from the edge of the n-contact.

The InGaN/GaN QW structures were grown on a c-plane sapphire using metal−organic chemical-vapor deposition in a Veeco D125 short-jar reactor. Trimethylgallium, trimethylindium, bis(cyclopentadienyl)magnesium, 200 ppm silane in N_2, and ammonia were used in H_2 and N_2 carrier gases to grow a 2−3 μm thick, Mg-doped, p-type GaN layer; a 3 nm thick InGaN QW; and a final, 3 nm thick Si-doped, n-type GaN layer. Growth was monitored using in situ reflectance,[13,14] and temperature was monitored using two infrared pyrometers. The p-GaN wafer was thermally activated in the reactor prior to the QW regrowth.

Electrical contacts were deposited by electron beam evaporation using an interdigitated mask that comprised several different device-mesa and contact geometries, as shown in Figure 1c. We used Ti/Al/Ni/Au and Pd/Au for n- and p-type contacts, respectively. p-type contacts were applied following plasma etching, which was used to reveal the hole-conducting GaN layer. Neither surface treatment on the n-side of the device nor contact anneals were performed to avoid damage to the InGaN QW and the thin, n-type barrier layer.

We used CdSe/ZnS core/shell NCs as color-selectable phosphors. NCs were prepared according to ref 15 and isolated from excess ligands by repeated precipitations with methanol. Following purification, the NCs were dissolved in toluene and spin-coated as a single monolayer onto an n-type layer of the GaN LED (the spin speed and the acceleration were 3000 rpm and 300 rpm/s, respectively). The NC photoluminescence (PL) quantum yield in solution (QY_{NC}^{sol}) was 60%, which was reduced to $QY_{NC}^{film} \approx 35\%$ in the monolayer (as derived from the comparison of PL dynamics for the solution and the monolayer samples). The reduced emission QY upon NC film formation occurs mainly because of inter-NC interactions[16] that can lead to exciton transfer from emitting to nonemitting NCs. The comparison of QYs for the solution and film samples indicates that on average each photoexcited exciton experiences one ET step within the monolayer before emitting a photon; in this case $QY_{NC}^{film} \approx (QY_{NC}^{sol})$,[2] which approximately describes the relationship between experimentally measured QYs.

Initially we studied the QW structure without the NC layer. Depending on the type of electronic excitations in a QW (free electron−hole pairs vs excitons), the radiative decay rate and the energy transfer rate are either independent of carrier density (electrons and holes are bound into excitons) or scale linearly with it (electrons and holes exist as free, independent particles).[4,12] To determine the nature of QW excitations, we investigated the relaxation characteristics of PL following QW excitation with 50-ps, 402-nm pulses derived from a pulsed diode laser (time-resolved measurements were performed using a time-correlated single-photon counting system). We also analyzed the dependence of the QW electroluminescence (EL) intensity on driving current.

Time-resolved QW PL studies indicate that the total relaxation rate is pump intensity independent and is ca. 2.6 ns^{-1} (Figure 2a). This rate is much faster than reported radiative rates (<0.5 ns^{-1}),[12] indicating that carrier recombination in our QW structures is dominated by nonradiative losses; hence, under stationary conditions the carrier density in the QW, n_{QW}, is simply proportional to the carrier generation rate, j, which scales linearly with the driving current: $n_{QW} \approx (k_{QW}^{nr})^{-1} j$, where k_{QW}^{nr} is the density-independent nonradiative decay rate (see eq 1 below).

The QW EL studies indicate that at moderate injection levels (before the onset of saturation) the emission intensity scales as a square of the driving current (Figure 2b). This result suggests quadratic scaling of the EL intensity with regard to n_{QW}. Such scaling further implies that the carrier radiative decay occurs via a bimolecular process, which is a

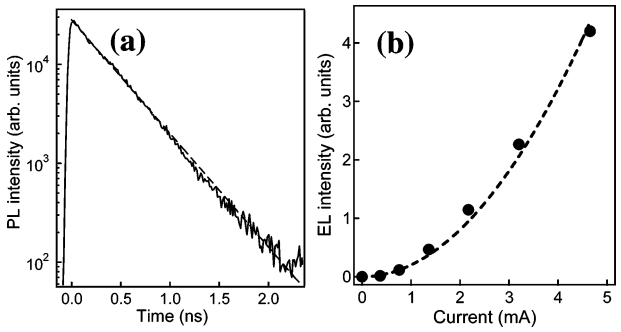

Figure 2. (a) Time-resolved QW PL taken at 415 nm. The PL decay is a single exponential with a decay rate of 2.6 ns^{-1} (dashed line). (b) EL of the QW device as a function of the driving current. The dashed line is a quadratic fit to the measured data.

signature of free electron−hole pair recombination. This analysis establishes that carriers in our QW structures are present not in the form of excitons but in the form of unbound electrons and holes, indicating that both radiative recombination and ET rates should scale linearly with carrier density.[4,12]

Next, we investigated hybrid QW−NC devices. We monitored their EL using a microscope coupled to a spectrometer, which allowed us to resolve both spatially and spectrally the emission from the area around the n-contact (see Figure 1b). All measurements were performed at moderate current levels of a few milliamperes to reduce local heating and the effect of emission intensity saturation. In the measured spectra, in addition to the QW band at ~420 nm, we clearly observed an NC band at 590 nm (Figure 3). The ratio between the measured NC and QW emission intensities is 13%, and it does not depend significantly on the driving current (inset of Figure 3) and, hence, excitation density in the QW (n_{QW}).

A useful characteristic of a color-conversion device is the color-conversion efficiency, η_{cc}. For devices studied here, it can be defined as the ratio between the total NC emission intensity in the hybrid structure (I_{NC}) and the total QW emission intensity in the absence of the NCs (I^0_{QW}): $\eta_{cc} = I_{NC}/I^0_{QW}$. The measured NC/QW emission intensity ratio is approximately equal to η_{cc} because the QW emission is only weakly attenuated (by less than 3%) by absorption in the NC monolayer and, further, because of nearly identical angular distributions of the NC and the QW emission intensities. While a large dielectric contrast between air and GaN is expected to have a significant effect on the emission pattern of near-interface dipoles, it influences the emission from the NCs and the QWs in a nearly identical way. Specifically, as shown in ref 17, if the dipole is in the immediate vicinity of the interface (i.e., at distances that are much shorter than the wavelength of light), the angular distribution of the emitted radiation is independent of whether the dipole is located in the high- or the low-index medium. These considerations imply that while we only measure the ratio of the NC to QW emission intensities for one specific direction, the ratio of total intensities (integrated over all angles) will be nearly the same.

To determine the origin of the NC emission, we compare the experimental color conversion efficiency with efficiency

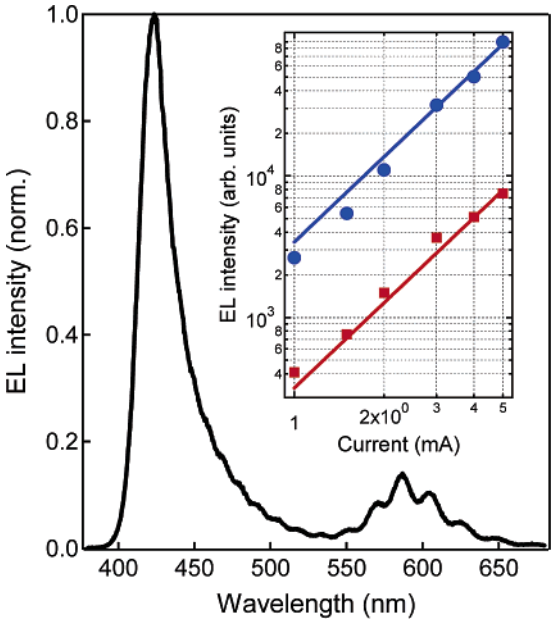

Figure 3. EL spectra (2 mA driving current) displaying both QW (420 nm) and NC (590 nm) emission bands (oscillations in the spectra are due to interference in the LED multilayer structure). Inset: QW (blue solid circles) and NC (red squares) emission intensities vs driving current, indicating that color-conversion efficiency (approximately the ratio of the two intensities) is independent of current. The straight lines are quadratic fits to the measured data.

values expected for ET. Further, we also evaluate a potential contribution to the NC emission from a traditional absorption−re-emission mechanism for NC activation. Although we consider the specific case of an InGaN QW LED as the primary light source and NCs as the phosphor materials, the discussion below is general and is applicable to other types of primary light sources and/or phosphor materials.

The QW carrier density in the absence of NCs, $n_{QW}{}^0$, is determined by the following rate equation

$$\frac{dn^0_{QW}}{dt} = j - k_{QW}n^0_{QW} \quad (1)$$

in which k_{QW} is the total decay rate in the QW, which accounts for both radiative and nonradiative losses: $k_{QW} = k^{rad}_{QW} + k^{nr}_{QW}$. Upon deposition of NCs on top of the QW, ET from the QW to the NCs introduces an additional relaxation channel with rate k_{ET} (a theoretical analysis of energy transfer rates in a QW/NC system in different temperature and excitation-density regimes can be found in ref 12). Corresponding rate equations for the QW and the NC excitations are

$$\frac{dn_{QW}}{dt} = j - k_{ET}n_{QW} - k_{QW}n_{QW} \quad (2)$$

$$\frac{dn_{NC}}{dt} = k_{ET}n_{QW} - k_{NC}n_{NC} \quad (3)$$

in which n_{NC} is the carrier density in NCs and k_{NC} is the

total decay rate of the NC excitations, which is the sum of radiative (k_{NC}^{rad}) and nonradiative (k_{NC}^{nr}) decay rates.

The NC PL intensity can be expressed as follows: $I_{NC} = k_{NC}^{rad} n_{NC}$. Assuming stationary conditions [d(...)/dt = 0] and combining eqs 1, 2, and 3, we obtain

$$I_{NC} = QY_{NC}^{film} I_{QW}^{0} \frac{k_{ET}}{k_{QW}^{rad} + QY_{QW} k_{ET}} = QY_{NC}^{film} I_{QW} \frac{k_{ET}}{k_{QW}^{rad}} \quad (4)$$

in which $I_{QW} = k_{QW}^{rad} n_{QW}$, and $QY_{NC}^{film} = k_{NC}^{rad}/k_{NC}$ and $QY_{QW} = k_{QW}^{rad}/k_{QW}$ are the emission quantum yields of the NC film and the QW, respectively. Finally, we calculate the color conversion efficiency

$$\eta_{cc} = \frac{I_{NC}}{I_{QW}^{0}} = QY_{NC}^{film} \frac{k_{ET}}{k_{QW}^{rad} + QY_{QW} k_{ET}} \quad (5)$$

As was discussed previously, for samples studied in this work, $k_{QW}^{nr} \gg k_{QW}^{rad}$ and, therefore, $QY_{QW} \ll 1$. Furthermore, taking into account that k_{ET} is on the order of or smaller than k_{QW}^{rad} (see quantitative analysis below), we can simplify eq 5 as

$$\eta_{cc} \approx QY_{NC}^{film} \frac{k_{ET}}{k_{QW}^{rad}} \quad (6)$$

One interesting implication of eq 6 is that the color conversion efficiency is dependent not on the total decay rate of QW excitations but only on their radiative decay rate. This type of dependence simplifies the control of η_{cc} in device structures because while k_{QW}^{rad} can be engineered in a predictable way,[12] the total rate, to which nonradiative losses also contribute, is much more difficult to control.

We use eq 6 to compare the measured color conversion efficiency with the one expected for the ET mechanism. In our previous optical study[4] with smaller NCs (core radius was 1.9 nm, shell thickness was 0.6 nm, ligand length was 1.1 nm, NC surface density was 2×10^{12} cm^{-2}, QW top barrier layer thickness was 3 nm, and the QW half width was 1.5 nm), we found that the ratio between ET and radiative decay rates, k_{ET}/k_{QW}^{rad}, was 1.33. We use this value to estimate k_{ET}/k_{QW}^{rad} in the present structures by scaling k_{ET} to account for the difference in the QW−NC separation, d, and the NC surface density. According to refs 4 and 12, the ET rate scales as d^{-4} and is proportional to the NC surface density. Taking into account the parameters of our present devices (NC core radius is 2.1 nm, shell thickness is 0.6 nm, ligand length is 2 nm, NC surface density is 1.2×10^{12} cm^{-2}, QW top barrier layer thickness is 3 nm, and the QW half width is 1.5 nm), we find $k_{ET}/k_{QW}^{rad} = 0.5$. Finally using QY_{NC}^{film} of 35%, we estimate from eq 6 a color conversion efficiency of 17%, which is close to the experimental value of 13%.

Next we evaluate a potential contribution to the measured NC emission intensity from a traditional absorption−re-emission color-conversion mechanism. Initially we consider "direct" excitation by the QW radiation emitted in the direction of the NCs (i.e., in the direction of the detector used in spectral measurements). The contribution from this process can be calculated based on the product of the NC monolayer absorbance ($A_{NC} = 0.025$) and the NC quantum yield (35%), which yields a conversion efficiency of less than 1%. Another potential contribution comes from activation of NCs by waveguided modes excited by the QW emission that is coupled into GaN (i.e., in the direction that is opposite to the detector). On the basis of the calculated angular distribution of the QW emission[18] and the measured absorption coefficient of the p-GaN layer ($\sim$1200 cm^{-1}), we estimate that NC excitation by the waveguided modes can, in principle, result in $\sim$3.5% color-conversion efficiency. These considerations imply that the absorption−re-emission mechanism alone cannot explain the measured values of η_{cc}, which provides strong evidence that the major fraction of the NC emission in our structures is activated by nonradiative ET from the QW. Taking into account a potential contribution from absorption−re-emission, we can estimate that the color-conversion efficiency produced by the ET process in our single-NC-layer structures is nearly 10%.

An interesting aspect of the ET color-conversion mechanism is that it can be used to significantly improve the absolute external quantum efficiency of phosphor-based emitters by reducing, e.g., losses resulting from nonradiative recombination in the LED and incomplete absorption by the phosphor. Furthermore, because the ET process is very efficient, even for thin, optically transparent acceptor layers, it can also eliminate losses caused by reabsorption and/or scattering of secondary photons in the phosphor medium itself.

In conclusion, we have demonstrated an LED structure in which CdSe NCs are excited by nonradiative ET from an electrically driven InGaN/GaN QW. The NCs act as efficient color converters of the QW emission. The measured color-conversion efficiency is 13%, which is significantly higher than the values expected for a mechanism based on absorption−re-emission. By elimination of several intermediate steps of the traditional color-conversion scheme, the ET mechanism can provide a significant reduction in losses during the color-conversion process. Another attractive feature of the ET scheme is that it can also produce improved efficiency compared to a stand-alone LED. Specifically, if the ET rate is sufficiently high compared to the rate of nonradiative losses in the QW, the majority of excitations can be "rescued" from nonradiative recombination by transferring them into the phosphor, which then efficiently converts them into photons. This consideration implies that the ET approach can produce high overall quantum efficiencies, even in the case of moderately efficient LEDs with thin QW barriers adjusted to optimize the ET rate.

Acknowledgment. This work was supported by the Technology Transfer Maturation Funds at Los Alamos National Laboratory and the Chemical Sciences, Biosciences, and Geosciences Division of the Office of Basic Energy Sciences, Office of Science, U.S. Department of Energy.

References

(1) Agranovich, V. M.; La Rocca, G. C.; Bassani, F. *JETP Lett.* **1997**, *66*, 748−751.
(2) Basko, D.; La Rocca, G. C.; Bassani, F.; Agranovich, V. M. *Eur. Phys. J. B* **1999**, *8*, 353−362.
(3) Agranovich, V. M.; Basko, D. M.; La Rocca, G. C.; Bassani, F. *Synth. Met.* **2001**, *116*, 349−351.
(4) Achermann, M.; Petruska, M. A.; Kos, S.; Smith, D. L.; Koleske, D. D.; Klimov, V. I. *Nature* **2004**, *429*, 642−646.
(5) Colvin, V.; Schlamp, M.; Alivisatos, A. *Nature* **1994**, *370*, 354−357.
(6) Schlamp, M. C.; Peng, X. G.; Alivisatos, A. P. *J. Appl. Phys.* **1997**, *82*, 5837−5842.
(7) Dabbousi, B. O.; Bawendi, M. G.; Onitsuka, O.; Rubner, M. F. *Appl. Phys. Lett.* **1995**, *66*, 1316−1318.
(8) Tessler, N.; Medvedev, V.; Kazes, M.; Kan, S.; Banin, U. *Science* **2002**, *295*, 1506−1508.
(9) Bakueva, L.; Musikhin, S.; Hines, M. A.; Chang, T.-W. F.; Tzolov, M.; Scholes, G. D.; Sargent, E. H. *Appl. Phys. Lett.* **2003**, *82*, 2895−2897.
(10) Coe, S.; Woo, W.-K.; Bawendi, M.; Bulovic, V. *Nature* **2002**, *420*, 800−803.
(11) Mueller, A. H.; Petruska, M. A.; Achermann, M.; Werder, D. J.; Akhadov, E. A.; Koleske, D. D.; Hoffbauer, M. A.; Klimov, V. I. *Nano Lett.* **2005**, *5*, 1039−1044.
(12) Kos, S.; Achermann, M.; Klimov, V. I.; Smith, D. L. *Phys. Rev. B* **2005**, *71*, 205309.
(13) Koleske, D. D.; Fischer, A. J.; Allerman, A. A.; Mitchell, C. C.; Cross, K. C.; Kurtz, S. R.; Figiel, J. J.; Fullmer, K. W.; Breiland, W. G. *Appl. Phys. Lett.* **2002**, *81*, 1940−1942.
(14) Koleske, D. D.; Coltrin, M. E.; Russell, M. J. *J. Cryst. Growth* **2005**, *279*, 37−54.
(15) Fisher, B. R.; Eisler, H.-J.; Stott, N. E.; Bawendi, M. G. *J. Phys. Chem. B* **2004**, *108*, 143−148.
(16) Achermann, M.; Petruska, M. A.; Crooker, S. A.; Klimov, V. I. *J. Phys. Chem. B* **2003**, *107*, 13782−13787.
(17) Lukosz, W.; Kunz, R. E. *J. Opt. Soc. Am.* **1977**, *67*, 1615−1619.
(18) Hellen, E. H.; Axelrod, D. *J. Opt. Soc. Am. B* **1987**, *4*, 337−350.

NL060392T